

MIT Open Access Articles

Determination of bandgap states in p-type $\text{In}_{0.49}\text{Ga}_{0.51}\text{P}$ grown on SiGe/Si and GaAs by deep level optical spectroscopy and deep level transient spectroscopy

The MIT Faculty has made this article openly available. **Please share** how this access benefits you. Your story matters.

Citation: Gonza#lez, M., A. M. Carlin, C. L. Dohrman, E. A. Fitzgerald, and S. A. Ringel. "Determination of bandgap states in p-type $\text{In}_{0.49}\text{Ga}_{0.51}\text{P}$ grown on SiGe/Si and GaAs by deep level optical spectroscopy and deep level transient spectroscopy." *Journal of Applied Physics* 109, no. 6 (2011): 063709. © 2011 American Institute of Physics

As Published: <http://dx.doi.org/10.1063/1.3559739>

Publisher: American Institute of Physics (AIP)

Persistent URL: <http://hdl.handle.net/1721.1/79619>

Version: Final published version: final published article, as it appeared in a journal, conference proceedings, or other formally published context

Terms of Use: Article is made available in accordance with the publisher's policy and may be subject to US copyright law. Please refer to the publisher's site for terms of use.



Determination of bandgap states in p-type $\text{In}_{0.49}\text{Ga}_{0.51}\text{P}$ grown on SiGe/Si and GaAs by deep level optical spectroscopy and deep level transient spectroscopy

M. González, A. M. Carlin, C. L. Dohrman, E. A. Fitzgerald, and S. A. Ringel

Citation: *J. Appl. Phys.* **109**, 063709 (2011); doi: 10.1063/1.3559739

View online: <http://dx.doi.org/10.1063/1.3559739>

View Table of Contents: <http://jap.aip.org/resource/1/JAPIAU/v109/i6>

Published by the AIP Publishing LLC.

Additional information on J. Appl. Phys.

Journal Homepage: <http://jap.aip.org/>

Journal Information: http://jap.aip.org/about/about_the_journal

Top downloads: http://jap.aip.org/features/most_downloaded

Information for Authors: <http://jap.aip.org/authors>

ADVERTISEMENT



The advertisement banner features a green and yellow background with abstract wavy lines. On the left, the text 'AIPAdvances' is displayed in a stylized font, with 'AIP' in blue and 'Advances' in green, followed by a series of orange dots. On the right, a circular seal contains the text 'Now Indexed in Thomson Reuters Databases'. Below this, a blue horizontal bar contains the text 'Explore AIP's open access journal:' followed by a bulleted list of features.

AIPAdvances

Now Indexed in
Thomson Reuters
Databases

Explore AIP's open access journal:

- Rapid publication
- Article-level metrics
- Post-publication rating and commenting

Determination of bandgap states in p-type $\text{In}_{0.49}\text{Ga}_{0.51}\text{P}$ grown on SiGe/Si and GaAs by deep level optical spectroscopy and deep level transient spectroscopy

M. González,^{1,a)} A. M. Carlin,¹ C. L. Dohrman,² E. A. Fitzgerald,² and S. A. Ringel^{1,b)}

¹The Ohio State University, Department of Electrical and Computer Engineering, Columbus, Ohio 43210, USA

²Department of Material Science and Engineering, Massachusetts Institute of Technology, Cambridge, Massachusetts 02139, USA

(Received 30 September 2010; accepted 29 January 2011; published online 22 March 2011)

The presence and properties of traps in p-type $\text{In}_{0.49}\text{Ga}_{0.51}\text{P}$ grown on low dislocation density, metamorphic Ge/SiGe/Si substrates and GaAs substrates were determined using deep level transient spectroscopy (DLTS) and deep level optical spectroscopy (DLOS) leading to the quantification of trap behavior throughout the entire 1.9 eV bandgap of the $\text{In}_{0.49}\text{Ga}_{0.51}\text{P}$ material as a function of substrate. Thermal emission-based DLTS revealed a single hole trap at $E_v + 0.71$ eV for growth on both lattice matched and mismatched substrates with similar concentrations. Complementary, optical emission-based DLOS measurements detected bandgap states at $E_v + 1.18$ eV, $E_v + 1.36$ eV, and $E_v + 1.78$ eV for p-type $\text{In}_{0.49}\text{Ga}_{0.51}\text{P}$ grown on both substrate types. The total concentration of the DLOS-detected states was found to comprise approximately 80% of the entire trap concentration in p-type $\text{In}_{0.49}\text{Ga}_{0.51}\text{P}$ bandgap. This relatively high concentration of above midgap levels may be of great significance for minority carrier devices that utilize p-type $\text{In}_{0.49}\text{Ga}_{0.51}\text{P}$ (such as high efficiency III–V multijunction solar cells) since their position in the bandgap and high concentrations suggest that strong minority carrier electron trapping behavior can be expected. The primary effect of substituting the GaAs substrate by Ge/SiGe/Si is to increase the concentration of these states by a factor of 2–3, with no additional levels detected due to the replacement by the Si-based substrates, indicating that all detected traps are native to the epitaxial $\text{In}_{0.49}\text{Ga}_{0.51}\text{P}$ material (regardless of the substrate), but whose concentrations appear to be influenced by dislocation density. © 2011 American Institute of Physics. [doi:10.1063/1.3559739]

I. INTRODUCTION

The integration of III–V material and devices with a Si substrate through the use of $\text{Si}_{1-x}\text{Ge}_x$ compositionally step graded buffers coupled with precise III–V/IV interface nucleation is of great technological promise as this approach has been shown to simultaneously reduce threading dislocation densities to low residual values, eliminate the formation of antiphase domains, and dramatically suppress interface diffusion and autodoping.^{1–5} Based on these initial materials studies, subsequent works established a variety of GaAs/Si devices via SiGe graded layers,^{6,7} which have now been extended to include monolithic integration of more advanced III–V structures on Si that incorporate wider bandgap III–V materials including InGaP/GaAs dual junction solar cells,^{8,9} GaInP LEDs (Ref. 10), and visible red AlGaInP laser diodes.¹¹ As the number of applications where InGaP and its alloys are a fundamental part of the system continues to grow, the necessity to understand the impact of electronic defects that may be present within the bandgap of these III–P based materials grown on SiGe accrues, especially given the increased detrimental effect of deep levels within progressively larger bandgap semiconductors. This, coupled with the presence of low, but still residual density of threading disloca-

tions from the SiGe substrates makes knowledge of deep level defects and their distribution critical to advance any device performance and ultimately understand device reliability.

With this as motivation, we investigate the presence and properties of deep levels within $n^+\text{p}$ $\text{In}_{0.49}\text{Ga}_{0.51}\text{P}$ (InGaP) diodes grown on Ge/Si_xGe_{1-x}/Si substrates. At this composition disordered InGaP displays a bandgap of ~ 1.9 eV and is nominally lattice matched to both Ge/SiGe/Si (hereafter referred to as SiGe/Si) and GaAs substrates. With the purpose of discerning traps related to growth on the metamorphic SiGe/Si substrate, the signature and concentration of the traps in InGaP structures grown on SiGe/Si were measured and compared to those within identical structures grown on GaAs. Conventional thermal spectroscopy techniques such as deep level transient spectroscopy¹² (DLTS) were employed. In addition, and to circumvent practical experimental limitations inherent to the thermal nature of these techniques (which preclude complete trap spectrum analysis within the totality of the bandgap in wider bandgap materials) we utilize the method of deep level optical spectroscopy (DLOS).¹³ DLOS enables detection and analysis of deep levels with energy positions far deeper than can be detected by methods based on thermal stimulation such that, the combination of DLOS and DLTS can reveal trap states throughout the entire bandgap of these relatively wide bandgap materials. DLOS has proven invaluable for similar studies of even wider bandgap materials such as GaN or AlGaIn (Refs. 14–18).

^{a)}Currently at Global Defense Technology and Systems Inc. (GTEC), Crofton, MD, USA.

^{b)}Electronic mail: ringel@ece.osu.edu.

II. EXPERIMENTAL METHODS

$\text{In}_{0.49}\text{Ga}_{0.51}\text{P}$ diodes having n^+p configuration were grown on SiGe/Si and GaAs substrates by Molecular Beam Epitaxy (MBE) at a substrate temperature of 490 °C. Si and Be were used as n- and p-type dopants, respectively. The emitter layer of the diode structures was doped to a concentration of $1 \times 10^{18} \text{ cm}^{-3}$. The base layer was intentionally lightly doped to $\sim 5 \times 10^{16} \text{ cm}^{-3}$ to improve trap sensitivity. The thicknesses of the emitter and base layer were 0.5 and 2 μm , respectively. This configuration ensured that the depletion region probed by trap characterization methods is well within the p-type base layer. The diodes were capped with a $1 \times 10^{19} \text{ cm}^{-3}$ Si-doped 0.1 μm GaAs layer to improve ohmic contact adhesion and resistance. The GaAs cap layer was grown at 560 °C. The SiGe/Si substrates consisted of compositionally step-graded $\text{Si}_{1-x}\text{Ge}_x$ layers grown by ultra high vacuum chemical vapor deposition on Si wafers offcut 6° from the (100) orientation toward the nearest {111} plane.¹⁹ The final threading dislocation density of the fully relaxed Ge layer on SiGe/Si was $\sim 1 \times 10^6 \text{ cm}^{-2}$ as determined by etch pit density and plan view Transmission Electron Microscopy (TEM). Full details of SiGe epitaxy and structural characterization can be found in Ref. 19. The growth initiation and nucleation conditions used to achieve anti-phase domain free epitaxy on Ge terminated surfaces have been described in detail elsewhere.^{5,7} Identical control structures were grown on (100) GaAs substrates with the same offcut direction and magnitude to assess any role of the SiGe/Si substrate in the introduction of defects. After growth, conventional optical lithography was used to fabricate diode structures. Electron-beam metal evaporation was used to deposit Cr/Au and Ni/Ge/Au to provide p and n ohmic contacts, respectively. The diode structures were mesa isolated by wet chemical etching using HCl:DI solution at a 2:1 concentration, resulting in total diode areas ranging from 0.25 to 4 mm^2 .

High quality diodes on both SiGe and GaAs substrates were obtained with this process, as seen by the J-V characteristics in Fig. 1. The measured reverse current density at

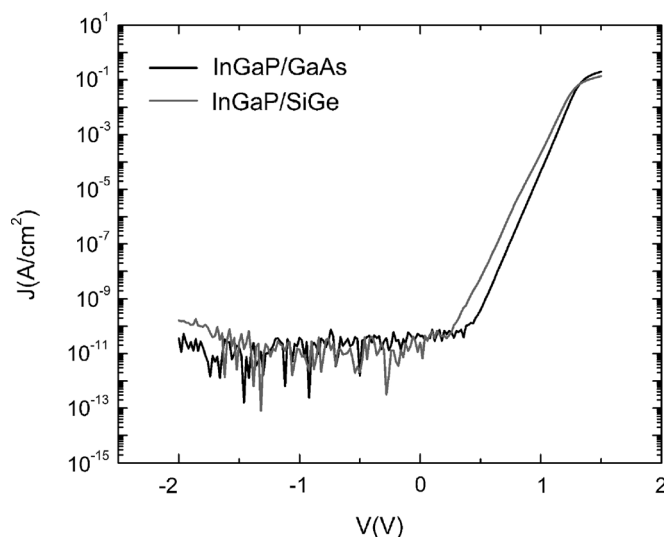


FIG. 1. J-V characteristics for InGaP diodes grown on SiGe/Si and GaAs substrates obtained at 300 K. The reverse bias leakage current was below the detection limit of 0.1 nA/cm^2 for both cases out to $\sim -2\text{V}$ reverse bias.

300 K of the InGaP diodes on both the SiGe/Si and GaAs substrates was below our measurement detection limit of 0.1 nA/cm^2 out to a reverse bias of $\sim -2\text{V}$ indicating that the diodes are well-suited for DLTS and DLOS experiments in a reasonable range of bias values. C-V measurements made on both samples confirmed a p-type doping concentration of $5 \times 10^{16} \text{ cm}^{-3}$ for the InGaP diode base so that a one sided junction approximation could be used. With this doping value and based on our instrumentation, the trap density detection limit is approximately $1 \times 10^{12} \text{ cm}^{-3}$.

All DLTS measurements were made using a quiescent reverse bias of -2V . A 10 ms filling pulse to -0.1V was used to fill traps in the p-type base with holes. The temperature range used for all DLTS measurements was ~ 100 to 400 K. Capacitance transients were obtained using a computer-controlled system including a function generator to provide trap filling, and a Boonton 7200 (1 MHz) capacitance meter along with a digital oscilloscope for averaging and recording the capacitance transient. The stored capacitance transient data as a function of temperature could then be analyzed by any standard method, such as boxcar averaging or more elaborate frequency domain methods.

DLOS measurements were made at 300 K following the approach described in Ref. 13. Here, the dependence on thermally stimulated emission of carriers from deep levels to observe carrier-detraping behavior (as is done for conventional DLTS) is replaced by optical stimulation of carriers trapped by bandgap states. The major advantage for characterizing deep level states in this fashion for semiconductors with relatively large bandgaps is that deep states (i.e., those with activation energies $> \sim 0.8\text{eV}$) including states present in the “minority carrier” half of the bandgap can be easily observed and analyzed. Using a combination of Xe arc and quartz-halogen lamps coupled to a monochromator, a tunable, monochromatic (with a bandpass ranging between 16 and 32 nm, corresponding to an energy resolution between 0.006 and 0.05 eV, depending on the wavelength and the grating used) optical source for direct deep level photo-stimulation is created and, for our setup, states with energies as far as $\sim 5.5\text{eV}$ from any band edge can be observed at room temperature. For InGaP, with its 1.9 eV bandgap, this is important since conventional DLTS can only observe states having energy positions less than approximately 1 eV from a band edge, and typically only the majority carrier band edge, which for our case of p-type material is the valence band edge. This means that midgap traps and those present in the upper half of the p-type InGaP bandgap, which typically would not be observed by DLTS, may now be evident. Since DLOS is performed so that the photo-stimulated carriers are sensed via changes in the depletion capacitance, many of the DLTS-based relationships to ascertain trap concentration remain valid. The primary (but fundamentally significant) difference is that, for DLOS, the optical cross section of a state is analyzed and this must be interpreted in the context of the depletion capacitance.

To perform DLOS measurements on the InGaP diodes, grid-type metal contacts were used and the top cap GaAs layer was etched with a $\text{NH}_4\text{OH}:\text{H}_2\text{O}_2:\text{DI}$ solution at 2:1:50 so that light could be coupled into the InGaP semiconductor.

As in DLTS, a -2 V quiescent reverse bias was used, with a trap filling pulse to -0.1 V for 10 ms. This was followed by a settling time for 30 s in the dark prior to optical excitation as a function of wavelength, which allows “faster” thermal emission transients emanating from relatively shallow traps (if present) to die out, ensuring that the data obtained via DLOS are due to photoexcitation. Note that all measurements reported here were done at 300 K, and this sets a limit on the minimum trap energy that can be seen by DLOS based on thermal emission rates at this temperature (lower measurement temperatures would translate to DLOS being able to sense traps with lower activation energies since the thermal emission rates reduce, but this is accomplished here by DLTS instead). Details on the theory as well as more complete descriptions of DLOS measurements can be found in Refs. 13 through 18.

III. RESULTS AND DISCUSSION

A. DLTS-detected traps in p-type InGaP grown on SiGe/Si and GaAs substrates

Figure 2(a) shows a comparison of typical DLTS spectra obtained for the n^+p InGaP diode structures grown on the SiGe/Si and GaAs substrates, and Table I shows the experimental values of the thermal activation energy, E_A (eV), thermal capture cross section σ_p (cm^2) and trap concentration, N_T (cm^{-3}). As seen, the spectra are quite similar with only one significant majority carrier hole trap detected in both samples located at an energy of $E_v + (0.71 \pm 0.01)$ eV. As shown in Fig. 2(b), where the measured Arrhenius plots associated with the $E_v + 0.71$ eV trap in each type of sample are plotted, the traps appear to be closely matched. This, coupled with the nearly identical concentration of this trap for both sample types, strongly suggests that the physical source for this trap is either a native defect or a common impurity present in the MBE-grown p-type InGaP. Indeed, there have been prior reports of a hole trap having an activation energy in the range of $E_v + (0.70 - 0.75)$ eV for Be-doped InGaP using gas source MBE.^{20,21} In addition, traps at $E_v + (0.70 - 0.73)$ eV have been found in electron and proton radiated p-type InGaP grown by metal-organic chemical vapor deposition, for which annealing studies attributed the physical origin to vacancies or interstitials.^{22–24} While associating the hole trap in this work with these earlier reports is speculative, the fact that this hole trap is widely observed does support the notion that its source is native to

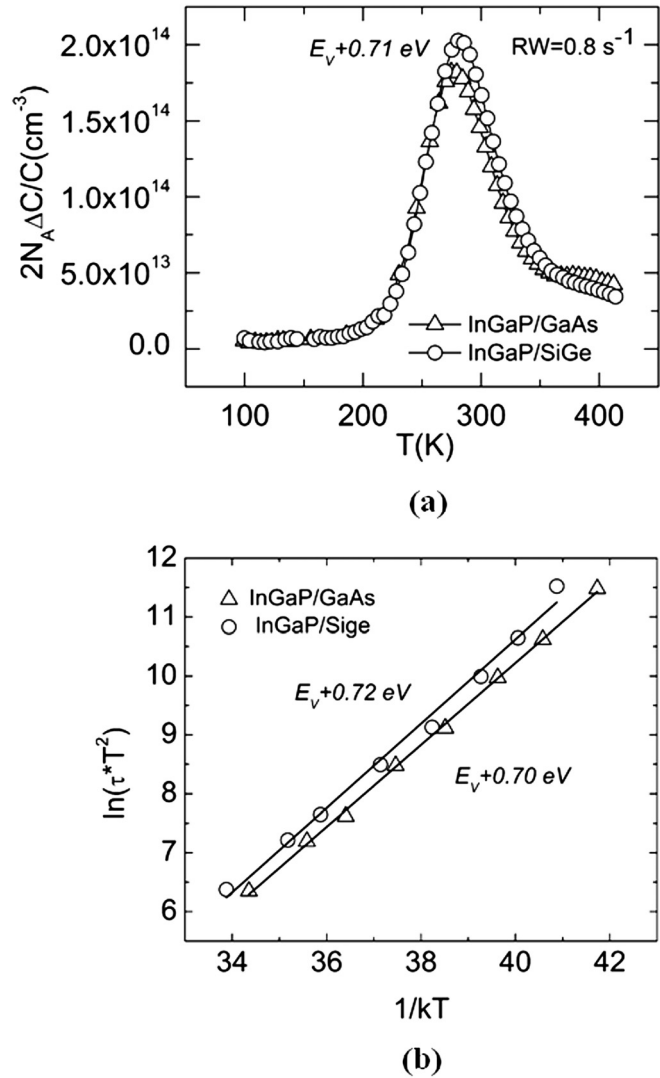


FIG. 2. (a) DLTS spectra obtained for identical n^+p InGaP diodes grown on SiGe/Si and GaAs substrates. The data shown corresponds to a measurement rate window of 0.8 s^{-1} . (b) DLTS data for a wide range of rate windows is shown in the usual Arrhenius format from which the activation energy and capture cross section are derived. These values are listed in Table I.

the material. Regardless of the physical source for this trap, DLTS reveals that there is no impact on the substitution of metamorphic SiGe/Si for GaAs as the substrate material from the viewpoint of traps that are detectable by DLTS, in spite of the residual density of threading dislocations for the former.

TABLE I. Trap parameters obtained from DLTS and DLOS measurements for bandgap states detected in p-type InGaP layers grown on both SiGe/Si and GaAs substrates.

	InGaP/SiGe			InGaP/GaAs		
	$E_T - E_v$ (eV)	σ_p (cm^{-2})	N_T (cm^{-3})	$E_T - E_v$ (eV)	σ_p (cm^{-2})	N_T (cm^{-3})
DLTS	0.72	2×10^{-13}	2.0×10^{14}	0.70	1.3×10^{-13}	1.8×10^{14}
DLOS	$E_T - E_v$ (eV)		N_T (cm^{-3})	$E_T - E_v$ (eV)		N_T (cm^{-3})
	1.18		2.2×10^{14}	1.18		1.4×10^{14}
	1.37		2.3×10^{14}	1.35		1.2×10^{14}
	1.78		9.0×10^{14}	1.79		2.9×10^{14}

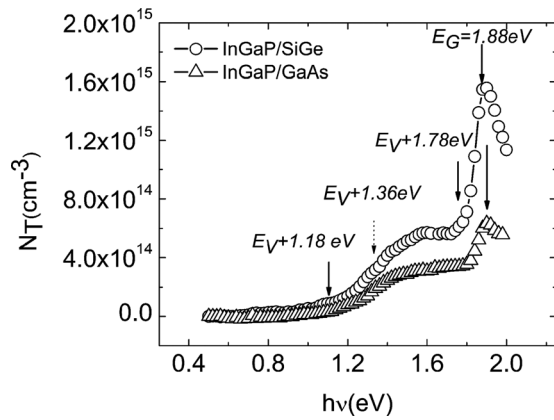


FIG. 3. Steady state photocapacitance spectra obtained at 300 K for p-InGaP grown on SiGe/Si and GaAs substrates. Three deep levels with photocapacitance onset energies at $E_v + 1.18$ eV, $E_v + 1.36$ eV, and $E_v + 1.78$ eV are observed for both sample types. The band edge is also identified as shown in the figure.

B. DLOS-detected traps in p-type InGaP grown on Ge/SiGe/Si and GaAs substrates

As mentioned above DLTS, being a method based on the analysis of thermally stimulated carrier emission from deep levels, is unable to observe traps with activation energies beyond ~ 1 eV at practical measurement temperatures. For the specific p-type InGaP samples here this means that bandgap states that might exist at energy levels near midgap and higher (closer to E_C) are not detectable by this method. DLOS instead is based on photostimulation; thus, it is only limited by the energy of the incident photons and the optical elements in the experimental apparatus. Figure 3 shows the steady state DLOS (i.e., photocapacitance) spectra obtained at room temperature for the same n⁺p InGaP structures grown on both SiGe/Si and GaAs substrates, but now using a grid front contact as described earlier. Onsets in the photocapacitance spectrum are indicative of carrier emission from a deep level to a band, with positive onsets indicating a transition to the majority carrier band, in this case the valence band edge. By illuminating for a sufficiently long time, saturation is reached and the trap concentration is given by the magnitude of the step height in the steady state spectrum for each onset. As seen, three additional bandgap states become immediately apparent that were not detected by DLTS, with onset energies at $E_v + 1.18$ eV, $E_v + 1.36$ eV, and $E_v + 1.78$ eV.

Before continuing with the DLOS analysis, it is important to explain why the $E_v + 0.71$ eV state detected by DLTS does not appear in the steady state photocapacitance spectrum, even when the optical source should excite this state. This is by design since, as mentioned before, DLOS photoexcitation is performed only after the sample is first held in the dark for 30 s, so that thermal transients die out. Equation 1 shows the expression for the hole thermal emission rate, e_p^{th} (or inversely the hole emission time constant, τ_p^{th}):

$$e_p^{th} = \frac{1}{\tau_p^{th}} = c_p^{th} N_V e^{E_v - E_T / kT} = \sigma_p^{th} v_p^{th} N_V e^{-(E_T - E_v) / kT}, \quad (1)$$

where c_p^{th} is the thermal capture rate for holes, v_p^{th} is the thermal velocity for holes, and N_V is the effective density of states in the valence band.

Considering a level located at 0.71 eV from the valence band with a thermal capture cross section of 1.5×10^{-13} cm² the emission time constant at room temperature is 0.1s, meaning that 63.2% of the trapped carriers will have returned to their free state in the valence band after 0.1 s. The 30 s settling time at the 300 K temperature used for DLOS gives ample time for the $E_v + 0.71$ eV state to emit its trapped holes prior to onset of DLOS excitation, being consistent with the spectra in Fig. 3.

The steady state photocapacitance spectra reveal that the concentration of these heretofore undetectable bandgap states are significantly greater than that of the hole trap found by conventional DLTS. As Table I shows, the total concentration of these DLOS-detected traps for InGaP/GaAs samples is $\sim 5.5 \times 10^{14}$ cm⁻³, compared with 2×10^{14} cm⁻³ for the hole trap at $E_v + 0.71$ eV, meaning that approximately 75% of the total trap density has been revealed by DLOS and had gone undetected by DLTS for p-type InGaP grown on GaAs. The situation is even more severe for the sample grown on SiGe/Si. Here the concentrations of these states are found to be $\sim 1.4 \times 10^{15}$ cm⁻³, which is more than 85% of the total trap concentration for these samples. Moreover, the fact that these states are either close to midgap, or reside in the minority band side of the bandgap, suggests that these levels could be serious limiters on minority carrier transport. In particular, these states would be of great importance for III-V photovoltaic applications where InGaP is the most common “top” sub-cell for the multijunction solar cells today and specifically, p-type InGaP is most commonly used as the base layer of these devices, where the majority of photocurrent collection is derived.^{25–28} The DLOS data also provides useful information regarding the impact of substituting the GaAs wafers by SiGe/Si substrates with their low, but not negligible, residual dislocation density. Whereas the DLTS data showed no impact for the dominant trap detected by that method, here there is a marked increase in the concentration of each state detected by DLOS, with the most pronounced (factor of three) increase for the level at $E_v + 1.78$ eV (the concentrations of the other states increased by a factor of 2 or less). However, just as in the case for DLTS, here we detect no new traps being introduced due to growth on SiGe/Si, only an increase in the concentrations of existing states. This is significant since it implies that the physical sources are native to the InGaP material and are not due to pure dislocation states. One possible explanation for the increase in concentrations is the potential for interactions between dislocations and native point defects present in the “nondislocated” regions of the layer. Dislocations and other extended defects are well known to act as gettering sites for point defects, which can be influenced by local strain fields and by coulombic interactions.^{29–31} Were such interactions to occur, an increase in average point defect density might happen over large areas (such as defined by the diode mesas) with the nondislocated field, where the point defect concentration will be determined by thermodynamic equilibrium arguments and must maintain an equilibrium concentration

(based on the growth conditions and growth phase diagram for InGaP independent of the presence of dislocations) and with local regions of higher concentrations being present at the dislocation cores. An alternative explanation might be the creation of point defects due to dislocation-dislocation interactions in the InGaP material as the dislocations terminated at the Ge surface of the SiGe/Si would now continue to migrate through the InGaP layer to reach the surface of the epitaxial layer. Additional work would be necessary to determine the basic reason for the observed increase, but the fact that the energy spectrum of traps is identical for both substrates demonstrates that the physical sources must be native point defects or common growth impurities, and cannot be due to the insertion of the SiGe/Si substrate.

Determination of the optical cross section associated with each state giving rise to the steady state photocapacitance onsets above, provides more detail on the nature of the physical defect. By measuring and analyzing the time dependence of the photocapacitance transient at each photon energy, the optical cross section for every deep level can be extracted by fitting the shape of the transient to established models, as described in earlier publications.^{32,33} Since the optical cross section is a distinct signature for a specific trap, this enables a path for defect identification. Determination of the optical cross section also allows more precise determination of the DLOS-measured energy levels since local lattice relaxation effects can be taken into account, which are not obvious from the steady state photocapacitance onsets. Two models are important for such fitting. For shallow to moderately deep states, optical cross sections typically follow the following temperature independent relationship:³⁴

$$\sigma^0 \propto \frac{(h\nu - E_0)^{3/2}}{(h\nu)^3} \quad (2)$$

where σ^0 is the optical cross section, $h\nu$ is the incoming photon energy, and E_0 is the ionization energy. For shallow levels, onsets in the steady state photocapacitance spectrum and energy thresholds (i.e., when $h\nu = E_0$) tend to coincide, and the steady state onset energies are indeed the true equilibrium energy levels. However, for deeper levels, or when phonons assist in ionization of defects (i.e., local lattice relaxation effects), it is often the case that this simple model breaks down. In this case, the energy spectrum of the optical cross section broadens due to thermal coupling and the steady state onsets will appear at energies $h\nu < E_0$. This effect is accounted for by the Chantre-Vicent-Bois model¹³ for which the optical cross section is expressed as:

$$\sigma^0 \propto \frac{E_0^2}{h\nu\sqrt{4k_B T \pi d_{FC}}} \int_1^{\infty} \sqrt{\frac{x-1}{E_0}} \frac{1}{[(x-1)/E_0 + m]} \times \exp\left[\frac{E_0^2(h\nu/E_0 - x)^2}{4k_B T \pi d_{FC}}\right] dx \quad (3)$$

Here, E_0 is the ionization energy, m is an adjustable mass term that accounts for band intermixing and d_{FC} is the Frank-Condon energy (or shift), which is a measure of the degree of local relaxation the lattice experiences upon

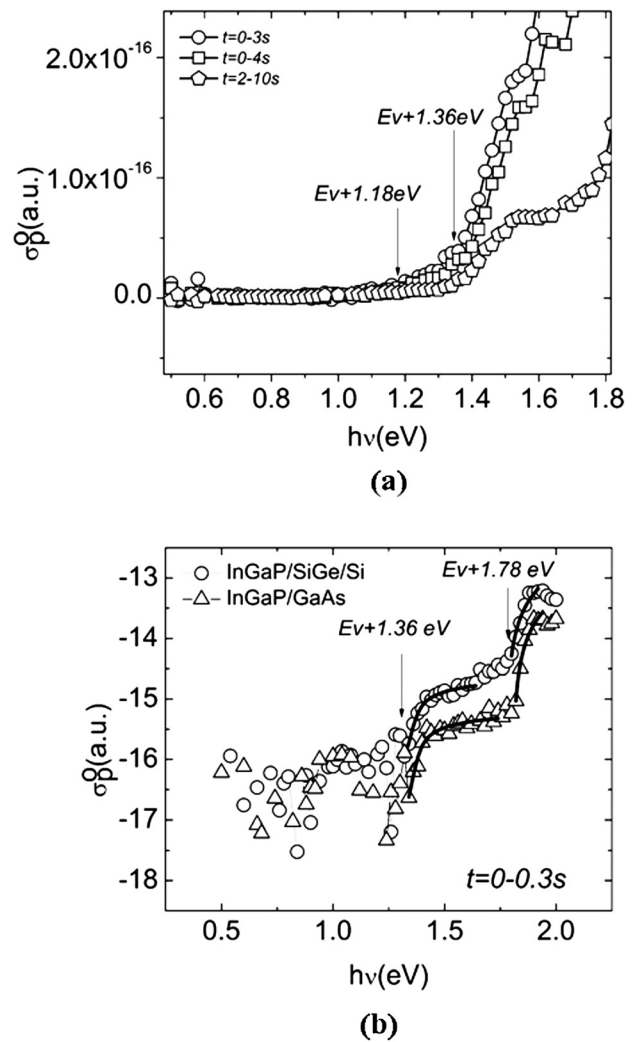


FIG. 4. (a) Derivative of the photocapacitance at different time intervals for InGaP/SiGe indicating energy ionization onsets at $E_v + 1.18$ eV and $E_v + 1.36$ eV. (b) Optical cross section spectra for p-InGaP grown on SiGe/Si for $t = 0-0.3$ s. Onsets at $E_v + 1.36$ eV and $E_v + 1.79$ eV are observed. Similar onsets are found for InGaP/GaAs.

capture or emission of a carrier. The value of E_0 and d_{FC} completely identifies the deep level signature, and avoids serious errors that can potentially be made when using the steady-state spectrum alone to identify true energy levels.

With previous theoretical considerations in mind, Fig. 4 shows the measured optical cross section data for both the InGaP/SiGe/Si and InGaP/GaAs samples, obtained under several representative time intervals. Because different levels might display different emission time constants (indicative of the different physical nature of the defects), many time intervals throughout the entire photocapacitance transient are acquired and analyzed, revealing the different levels in the bandgap. Figure 4(a) shows the derivative of the photocapacitance transient, which relates proportionally to the optical cross section (see Refs. 14–18), for time intervals (or rate windows) ranging from 0 to 10 s in which both the levels at $E_v + 1.18$ eV and $E_v + 1.36$ eV are observed. Figure 4(b) shows the cross section data for the specific rate window of 0–0.3 s. The data in Fig. 4(b) were fit to both models just described showing a close fit for the $E_v + 1.36$ eV and $E_v + 1.78$ eV. Similar fitting procedures were performed at

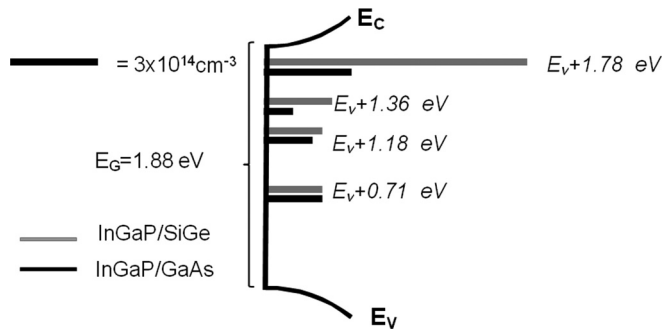


FIG. 5. Qualitative diagram of the deep level distribution within p-type InGaP/SiGe/Si and InGaP/GaAs bandgap representing the quantitative concentration of the levels within the bandgap. An overall higher trap concentration is observed for the sample grown on the metamorphic SiGe/Si substrate.

different rate windows for both InGaP/SiGe/Si and InGaP/GaAs samples with none of the states displaying a considerable Frank-Condon shift. Only one state, at $E_v + 1.36$ eV, displayed a measurable value of $\sim 0.03\text{--}0.05$ eV indicating negligible phonon interaction during the photo-excitation of these defects and negligible local strain surrounding the defects, suggestive that the physical sources for these states are likely to be point defects of InGaP.

Table I summarizes the measured trap data and parameters from both DLTS and DLOS for p-type InGaP grown on both substrate types. The diagram of Fig. 5 reveals the general distribution of bandgap states versus energy for p-type InGaP found in this work. As seen, the traps detected by DLOS that went undetected by DLTS are clearly dominant, and these states, due to their position in the bandgap, are likely to be significant factors for minority carrier (electron) transport through trapping and recombination-generation. This is expected to be particularly important for minority carrier devices, such as InGaP solar cells, for which efficient collection of minority carrier electrons is vital. Moreover, these upper bandgap states in the p-type InGaP appear to be more sensitive to the choice of substrate in this study, and the redistribution of their concentrations is depicted by the relative lengths of each line. As seen there is a differential impact of the substrate with respect to trap concentrations detected by DLOS, and the $E_v + 1.78$ eV level is far more sensitive to the choice of substrate than are the other states. This may give a clue to its physical source, which is a study beyond the scope of this work.

IV. CONCLUSIONS

Defect introduction within n^+p $\text{In}_{0.49}\text{Ga}_{0.51}\text{P}$ diodes grown on metamorphic SiGe/Si substrates was studied by DLTS and DLOS, which allowed the inspection of the total-ity of the ~ 1.9 eV InGaP bandgap. Similar studies were performed on identical samples grown on GaAs to assess the role of the residual threading dislocation density in the metamorphic InGaP/SiGe/Si sample. DLTS experiments showed the presence of a majority carrier hole trap at $E_v + 0.71$ eV within the p-base of both InGaP/SiGe/Si and InGaP/GaAs structures at similar trap concentrations, indicating that the physical source of this level is likely to be an intrinsic or ex-

trinsic defect native to the epitaxial material, and is not related to dislocations. Steady state as well as transient photocapacitance DLOS experiments, revealed the presence of three additional deep levels within the bandgap of both InGaP/SiGe/Si and InGaP/GaAs at $E_v + 1.18$ eV, $E_v + 1.36$ eV, and $E_v + 1.78$ eV, the source of which is again unlikely to be dislocation related since all the levels are present in both samples. The optical cross sections of the levels were extracted and fitted to theoretical models, showing negligible defect-lattice coupling with a maximum d_{FC} of $\sim 0.03\text{--}0.05$ for the $E_v + 1.36$ eV level. Results also showed that the low threading dislocation density present in the metamorphic structures does affect the trap concentration distribution within the bandgap, indicating the possibility of point defect-dislocation interactions in the metamorphic structures.

ACKNOWLEDGMENTS

All or parts of this work received support from the Army Research Office (DAAD 19-01-0588), Air Force Office of Scientific Research (FA9550-06-1-0557), the Ohio Wright Center for Photovoltaics Innovation and Commercialization, and the Intel Corporation.

- ¹J. A. Carlin, S. A. Ringel, E. A. Fitzgerald, and M. T. Bulsara, *Sol. Energy Mater. Sol. Cells* **66**, 621 (2001).
- ²R. M. Sieg, S. A. Ringel, S. M. Ting, E. A. Fitzgerald, and R. N. Sacks, *J. Electron. Mat.* **27**, 900 (1998).
- ³R. M. Sieg, S. A. Ringel, S. M. Ting, S. B. Samavedam, M. T. Currie, T. A. Langdo, and E. A. Fitzgerald, *J. Vac. Sci. Technol. B* **16**, 1471 (1998).
- ⁴R. M. Sieg, J. A. Carlin, J. J. Boeckl, S. A. Ringel, M. T. Currie, S. M. Ting, T. A. Langdo, G. Taraschi, E. A. Fitzgerald, and B. M. Keyes, *App. Phys. Lett.* **73**, 3111 (1998).
- ⁵J. A. Carlin, S. A. Ringel, E. A. Fitzgerald, M. T. Bulsara, and B. M. Keyes, *Appl. Phys. Lett.* **76**, 1884 (2000).
- ⁶J. A. Carlin, M. K. Hudait, S. A. Ringel, D. M. Wilt, E. B. Clark, C. W. Leitz, M. T. Currie, T. A. Langdo, and E. A. Fitzgerald, in *High Efficiency GaAs-on-Si Solar Cells Solar Cells With High Voc Using Graded GeSi Buffers*, Anchorage, Alaska, USA, 2000 [Proc. of 28th IEEE Photovoltaic Specialist Conf. (PVSC)].
- ⁷J. A. Carlin, S. A. Ringel, E. A. Fitzgerald, and M. T. Bulsara, *Prog. Photovolt.: Res. Appl.* **8**, 323 (2000).
- ⁸M. R. Lueck, C. L. Andre, A. J. Pitera, M. L. Lee, E. A. Fitzgerald, and S. A. Ringel, *IEEE Electron Device Lett.* **27** (2006).
- ⁹S. A. Ringel, C. L. Andre, M. R. Lueck, D. Isaacson, A. J. Pitera, E. A. Fitzgerald, and D. M. Wilt, in *III-V Multijunction Materials and Solar Cells on Engineered SiGe/Si substrates*, Boston, MA (2004).
- ¹⁰O. Kwon, J. J. Boeckl, M. L. Lee, A. J. Pitera, E. A. Fitzgerald, and S. A. Ringel, *J. Appl. Phys.* **97**, 034504 (2006).
- ¹¹O. Kwon, J. J. Boeckl, M. L. Lee, A. J. Pitera, E. A. Fitzgerald, and S. A. Ringel, *J. Appl. Phys.* **100**, 013103 (2006).
- ¹²D. V. Lang, *J. Appl. Phys.* **45**, 3023 (1974).
- ¹³A. Chantre, G. Vicent, and D. Bois, *Phys. Rev. B* **23**, (1981).
- ¹⁴A. R. Arehart, C. Poblentz, J. S. Speck, and S. A. Ringel, *J. Appl. Phys.* **107**, 054518 (2010).
- ¹⁵A. R. Arehart, A. Corrión, C. Poblentz, J. S. Speck, U. K. Mishra, and S. A. Ringel, *Appl. Phys. Lett.* **93**, 112101 (2008).
- ¹⁶A. M. Armstrong, A. R. Arehart, B. Moran, S. P. DenBaars, U. K. Mishra, J. S. Speck, and S. A. Ringel, *Appl. Phys. Lett.* **84**, 374 (2004).
- ¹⁷A. M. Armstrong, A. Chakraborty, J. S. Speck, S. P. DenBaars, U. K. Mishra, and S. A. Ringel, *Appl. Phys. Lett.* **89**, 262116 (2006).
- ¹⁸A. Hierro, A. R. Arehart, B. Heying, M. Hansen, U. K. Mishra, S. P. DenBaars, J. S. Speck, and S. A. Ringel, *Appl. Phys. Lett.* **80**, 805 (2002).
- ¹⁹M. T. Currie, S. B. Samavedam, T. A. Langdo, C. W. Leitz, and E. A. Fitzgerald, *App. Phys. Lett.* **72**, 1718 (1998).
- ²⁰J. H. Kim, S. J. Jo, J. W. Kim, and J. I. Song, *J. App. Phys* **89** 4407 (2001)
- ²¹H. S. Kim, M. J. Hafich, G. A. Patrizi, A. Nanda, T. J. Vogt, L. M. Woods, and G. Y. Robinson, *Elec. Lett.* **29**, 535 (1993).

- ²²A. Khan, M. Yamaguchi, J. C. Bourgoin, and T. Takamoto, *J. Appl. Phys.* **91**, 2391 (2002).
- ²³N. Dharmarasu, M. Yamaguchi, A. Khan, T. Takamoto, T. Ohshima, H. Itoh, M. Imaizumi, and S. Matsuda, *Physica B* **308–310**, 1181 (2001).
- ²⁴N. Dharmarasu, M. Yamaguchi, J. C. Bourgoin, T. Takamoto, T. Ohshima, I. Hisayoshi, M. Imaizumi, and S. Matsuda, *Appl. Phys. Lett.* **81**, 64 (2002).
- ²⁵F. Dimroth, *Phys. Stat. Sol. C* **3**, 373 (2006).
- ²⁶M. Stan, D. Aiken, B. Cho, A. Cornfeld, J. Diaz, V. Ley, A. Korostyshevsky, P. Patel, P. Sharps, and T. Varghese, *J. Cryst. Growth* **310**, 5204 (2008).
- ²⁷H. Yoon, M. Haddad, S. Mesropian, J. Yen, K. Edmonson, D. Law, R. R. King, D. Bhusari, A. Boca, and N. H. Karam, in *Progress of inverted metamorphic III–V solar cell development at Spectrolab*, San Diego, CA, p. 1 (2008).
- ²⁸R. R. King, D. C. Law, K. M. Edmondson, C. M. Fetzer, G. S. Kingsey, H. Yoon, S. A. Sherif, and N. H. Karam, *Appl. Phys. Lett.* **90**, 183516 (2007).
- ²⁹J. Ding, J. S. C. Chang, and M. Bujatti, *Appl. Phys. Lett.* **50**, 1089 (1989).
- ³⁰A. S. Salih, H. J. Kim, R. F. Davis and G. A. Rozgonyi, *Appl. Phys. Lett.* **46**, 419 (1984).
- ³¹T. Y. Tan, E. E. Gardner, and W. K. Tice, *Appl. Phys. Lett.* **30**, 175 (1977).
- ³²A. Armstrong, A. R. Arehart, D. Green, U. K. Mishra, J. S. Speck, and S. A. Ringel, *J. Appl. Phys.* **98**, 053704 (2005).
- ³³A. Armstrong, J. Caudill, A. Corrion, C. Poblenz, U. K. Mishra, J. S. Speck, and S. A. Ringel, *J. Appl. Phys.* **103**, 063722 (2008).
- ³⁴P. Blood and J. W. Orton, *The Electrical Characterization of Semiconductors: Majority Carriers and Electron States* (Oxford, England, 1992).